



## **Monitor Schemes for Angle and Position Tuning of the European XFEL Beamline Mirrors**

**Simon Wright**  
**St Catharine's College**  
**University of Cambridge**

**Supervisor: Dr. Jan Grünert**

### **Abstract:**

The European XFEL will produce ultrashort pulses of very intense radiation. To prepare this radiation for use, it must pass through a number of optical elements. The radiation shielding mirrors require a range of motion from 1-3 mrad, with an angular resolution of 0.01 mrad. Monitors are required to ensure the alignment of the elements. Two main detection schemes are investigated: a 'pencil beam' system in which the mirror is scanned through a small beam with the signal read by a photodiode, and an 'immersion' scheme in which the mirror is immersed in a wide beam, and the pattern viewed on a screen is analysed. An analysis of the degrees of freedom of the systems was carried out, to determine which parts must move, and the direction and accuracy of such movements required to produce the necessary resolution. Finally, laboratory experiments using optical light were carried out to demonstrate the viability of these schemes.

## Contents:

|  |    |
|--|----|
| 1. Introduction                        | 3  |
| 1.1. European XFEL                     | 3  |
| 1.2. Photon beam alignment             | 4  |
| 2. Monitor Schemes                     | 5  |
| 2.1. ‘Pencil beam’ setup               | 5  |
| 2.1.1. Theory for XFEL                 | 6  |
| 2.1.2. Experimental demonstration      | 8  |
| 2.2. ‘Immersion’ setup with screen     | 10 |
| 2.2.1. Theory for XFEL                 | 12 |
| 2.2.2. Experimental demonstration      | 12 |
| 2.3. ‘Immersion’ setup with photodiode | 14 |
| 2.3.1. Theory for XFEL                 | 14 |
| 2.3.2. Experimental demonstration      | 15 |
| 3. Comparison of Alignment Methods     | 17 |
| 4. Acknowledgements                    | 18 |
| 5. References                          | 18 |

# 1. Introduction

## 1.1. European XFEL

The European XFEL (X-Ray Free Electron Laser) is a €1.1 billion project under construction in Hamburg, due to be operational by 2015. It will be 3.4km long, running from the DESY site in Bahrenfeld to the site of the experimental hall, just south of the town of Schenefeld. Upon completion, the XFEL will revolutionise scientific research using ultrashort pulses of high intensity radiation. These pulses will cater for a range of scientific uses, from filming chemical reactions and the processes of magnetisation, to imaging the structure of biomolecules and investigating extreme states of matter.

The XFEL works by a process of Self-Amplified Spontaneous Emission (SASE). A beam of electrons is accelerated to a relativistic speed, before entering an undulator, which is made up of magnets of alternating polarity (Fig. 1.1). This causes the beam to ‘wiggle’, and due to its constant acceleration it emits photons. Since the electrons are travelling relativistically, it can ‘see’ the electromagnetic field from this radiation. The electrons then go through a second-order acceleration due to this in a process known as microbunching, which causes all the photons emitted to have the same wavelength. This causes a high intensity of photons with the same energy to be produced coherently. The XFEL has 33 undulator segments, each 5m long, to ensure that this process is maximised and that the beam is as collimated as possible.

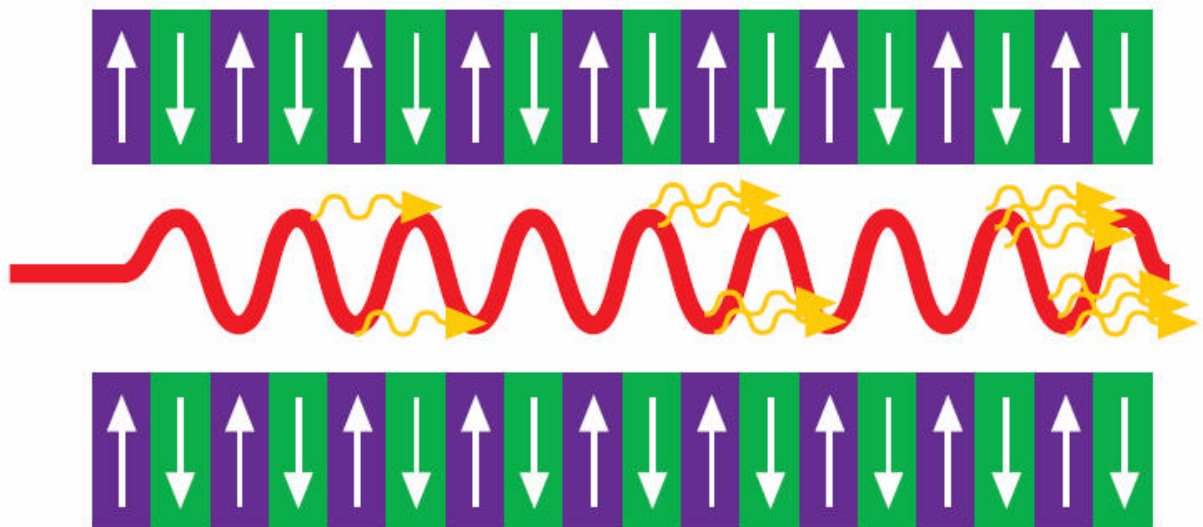


**Figure 1.1 – A sketch of an undulator, showing the magnets of alternating polarity and the oscillating path that the electrons take through it, producing coherent photons [1].**

In the XFEL, the electrons are accelerated to an energy up to 17.5 GeV, producing a beam of photons with a fundamental energy of 12.4 keV (equivalent to 0.1nm) in the SASE 1 beamline [2]. This provides the spatial resolution required to image biological structures to an atomic level.

There are two other XFELs; the Spring-8 Compact SASE Source (SCSS) in Japan, due for commissioning later in 2010, and the Linac Coherent Light Source (LCLS) in California, which commenced operation in 2009. What sets the European XFEL apart from these, aside from the fact it is capable of running at a slightly higher energy and hence lower wavelength, is the frequency of the pulses. The European XFEL is using a superconducting accelerator,

which enables it to pulse up to 27000 times every second, compared to 60 and 120 times at SCSS and LCLS respectively. Each pulse has a length of less than 100fs, giving an unprecedented temporal resolution at this intensity, allowing ‘movies’ of chemical reactions to be taken [3].

## 1.2. Photon beam alignment

In each beamline, there are numerous optical elements which ensure that the photon beam is as close as possible to the user specification when it reaches the sample.

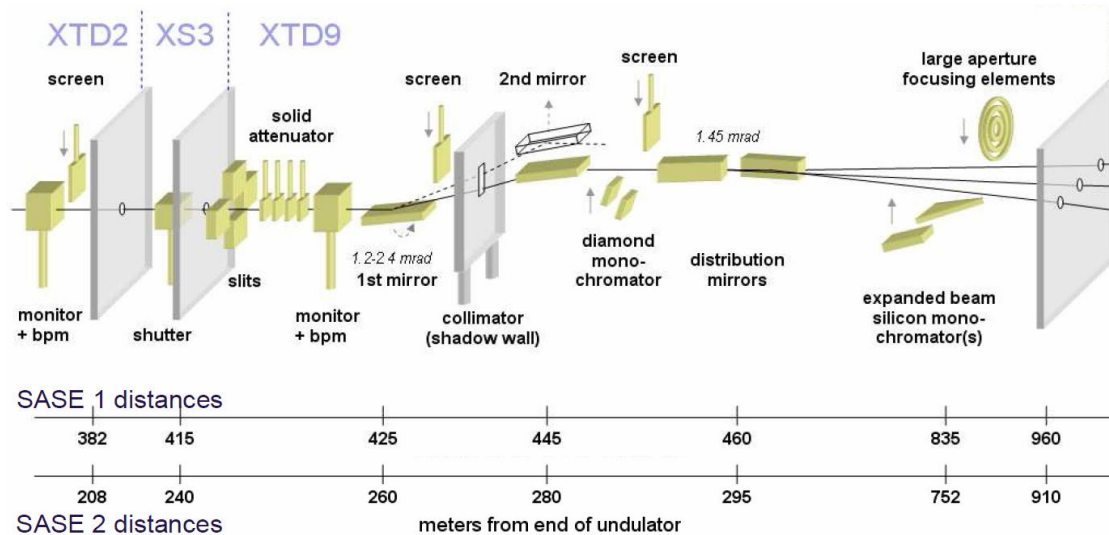


**Figure 1.2 – A schematic of the optical elements in the SASE 1 and SASE 2 beamlines. The screens are the monitoring devices under investigation here [4].**

There are two types of devices. Some, such as the monochromators and slits, change the properties of the beam, its energy and size respectively. Others, such as the monitors and screen, are diagnostic elements which ensure that the beam is in the correct place.

In my project, I focused on the diagnostics after the radiation shielding mirrors (named 1<sup>st</sup> and 2<sup>nd</sup> mirror in the schematic). These mirrors are necessary to remove all the higher harmonics from the beam, as these are at very high energies (upwards of 40 keV), and hence can put a very high heat load on the optical elements. At grazing incidence, x-rays can obtain total external reflection from the mirror. However, the reflectivity at a given angle sharply drops off at a critical energy for a given material. For a given range of angles, a suitable material can be chosen to place the energy cut-off between the fundamental energy and the higher harmonics. In this case, the angular range of motion is 1-3 mrad, and the material chosen is boron carbide (B<sub>4</sub>C).

The mirrors are very difficult to manufacture. The incoming photon beam, in full FEL operation, will be approximately 1mm in diameter. In order to avoid diffraction effects from cutting the edges of the beam off, the entire beam (at least up to 3 standard deviations of the Gaussian beam) must fall on the mirror. If the mirror is inclined at 1 mrad, its vertical projection must therefore be at least 1mm, meaning the mirror has to be of the order of 1m long. Also, local bumps will cause diffraction, so the mirror must be flat to a nanometer scale. Added to the fact that the mirror must be cooled to avoid bending due to heating, the scale of the problem is evident! But here I will assume the mirrors are perfect, and study schemes for their alignment.

## 2. Monitor Schemes

The specified accuracy for the alignment of the radiation shielding mirrors is that the beam from the first mirror must hit the centre of the second mirror to within  $200\mu\text{m}$  at a distance of 20m. This corresponds to an angular resolution of  $10\mu\text{rad}$ .

To achieve this, two different schemes were considered.

### 2.1. 'Pencil beam' setup

In this scheme, a small beam is incident upon the mirror, and reflected onto a fixed photodiode. The mirror is then scanned through the incident beam, from where the beam misses the top of mirror to where it passes underneath. The photodiode will measure a current depending on the different intensity of reflected radiation incident on it. The trace of this current with mirror position can then be analysed to determine the angle.

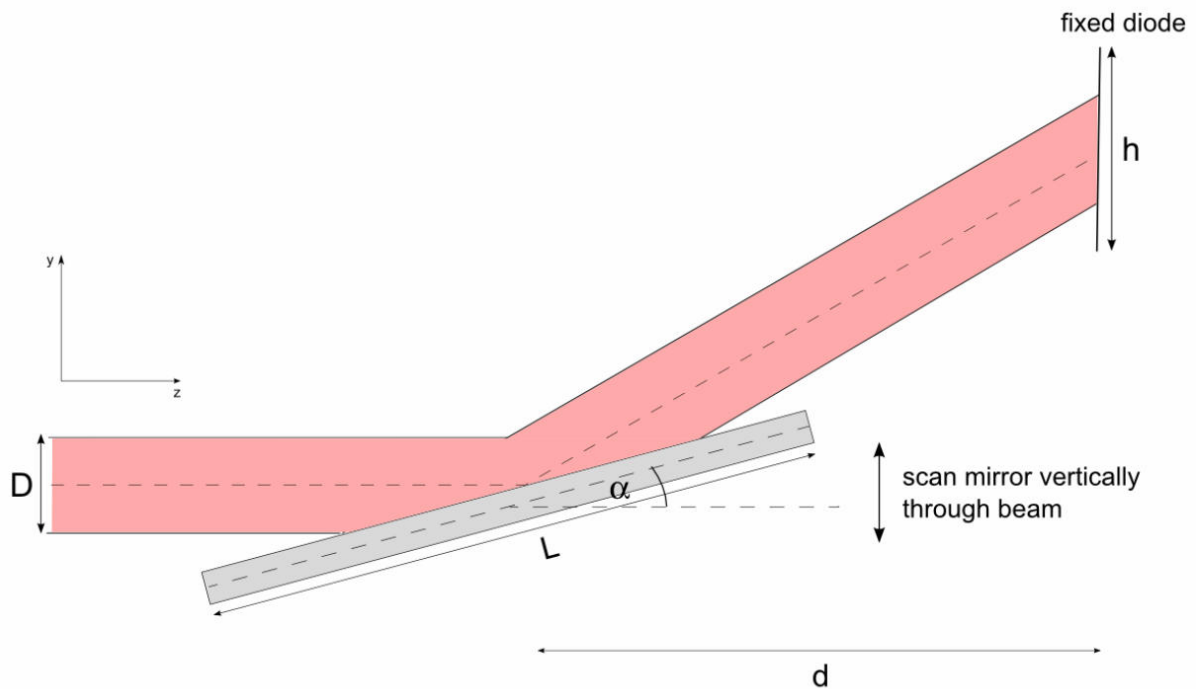


Figure 2.1a - A schematic of the setup for the pencil beam setup.  $D$  is the beam diameter,  $L$  is the length of the mirror,  $\alpha$  is the angle of the mirror to the incident beam,  $d$  is the distance of the diode from the centre of the mirror, and  $h$  is the height of the diode. The incident beam is in the  $z$ -direction.

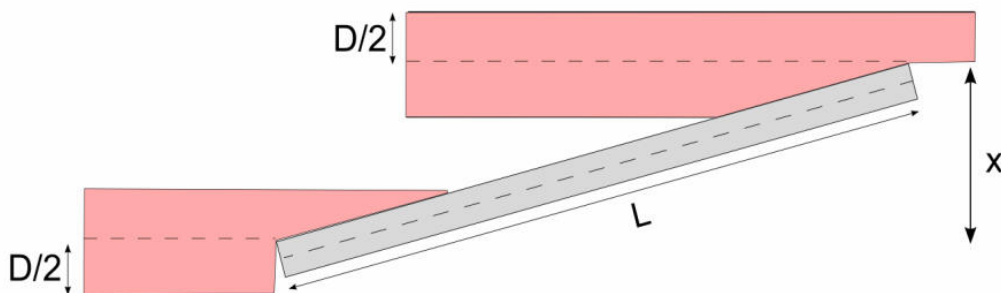


Figure 2.1b – The FWHM of the trace,  $x$ , is used to calculate the angle of the mirror.

### 2.1.1. Theory for XFEL

The determination of the angle is quite simple. As seen in Fig. 2.1b, the points at half the maximum intensity correspond to half the beam being reflected and half passing over or under the mirror. As a result, the FWHM (full width at half-maximum), denoted  $x$ , of the trace gives the projection of the mirror in the transverse direction (the  $y$  direction as marked in Fig. 2.1a).

Since the length of the mirror is known, the angle can be calculated simply by  $\sin \alpha = \frac{x}{L}$ .

Fig. 2.1c gives an example of the trace that should be seen by the photodiode. It has a characteristic top-hat shape from where the full beam is incident on the mirror, meaning that the maximum intensity value is easy to find. It also provides a method for centring the beam in the mirror after the angular alignment, as the mirror is moved to the centre of the plateau. However, there are limitations to this alignment method which can cause false traces to be observed.

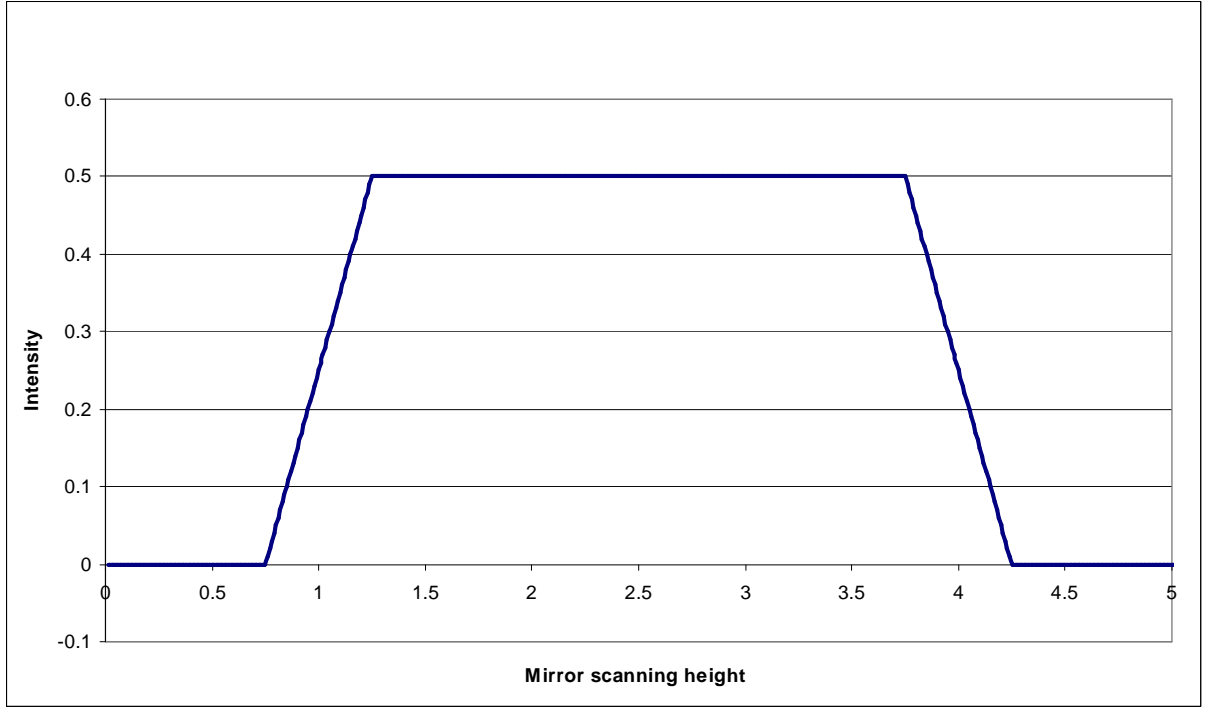


**Figure 2.1c – The nominal example trace for  $\alpha = 3$  mrad,  $h = 10$ mm,  $y_d = 8$ mm. In all these example traces,  $y_b = 2.5$ mm, and  $d = 1$ m.**

The first limitation is a constraint on the size of the diode. If the diode is too small, the beam will move off the edge of the diode will still being fully incident on the mirror, causing the photocurrent to decrease. This will obviously give a FWHM which is too small, and the same effect occurs when the diode is misaligned (Fig 2.1d-e). The condition to avoid this scenario is  $h > L \tan 2\alpha \cos \alpha + 2y_{off}$ , where  $y_{off} = |y_d - (y_b + d \tan 2\alpha)|$ ,  $y_d$  is the  $y$ -position of the centre of the diode and  $y_b$  is the  $y$ -position of the beam.

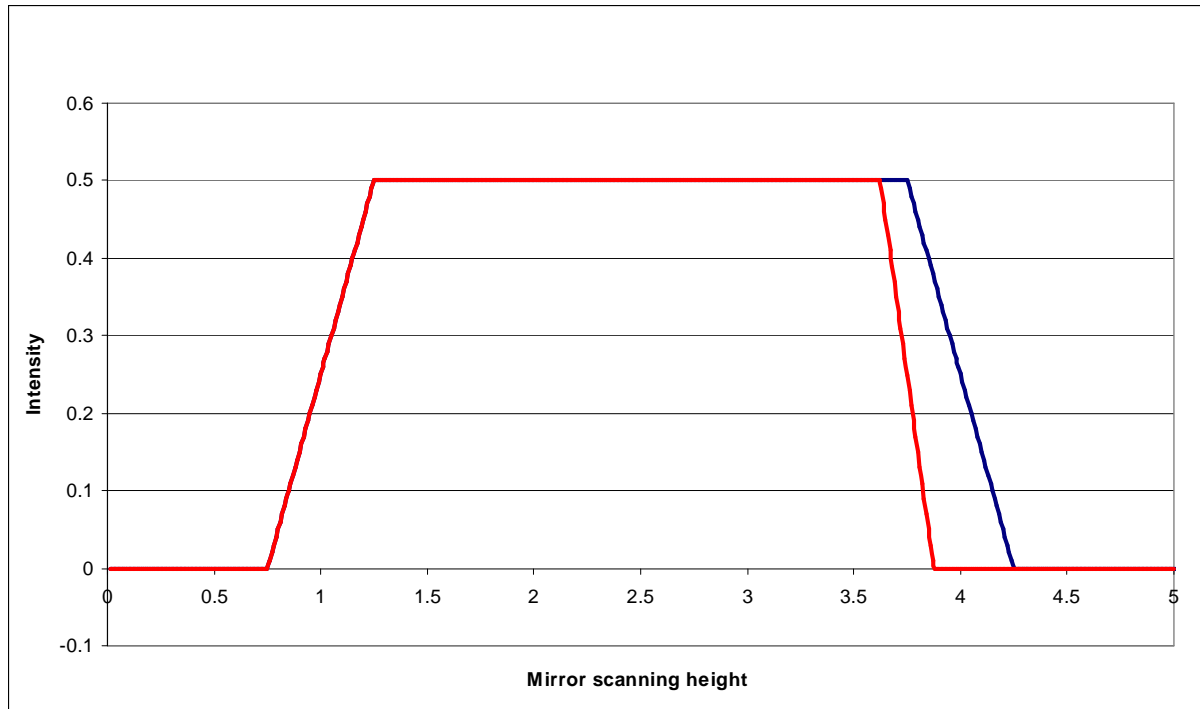


Figure 2.1d – The red trace represents the misaligned diode –  $\alpha = 3$  mrad,  $h = 10$ mm,  $y_d = 6$ mm. The trace is obviously cut-off on the right-hand side.

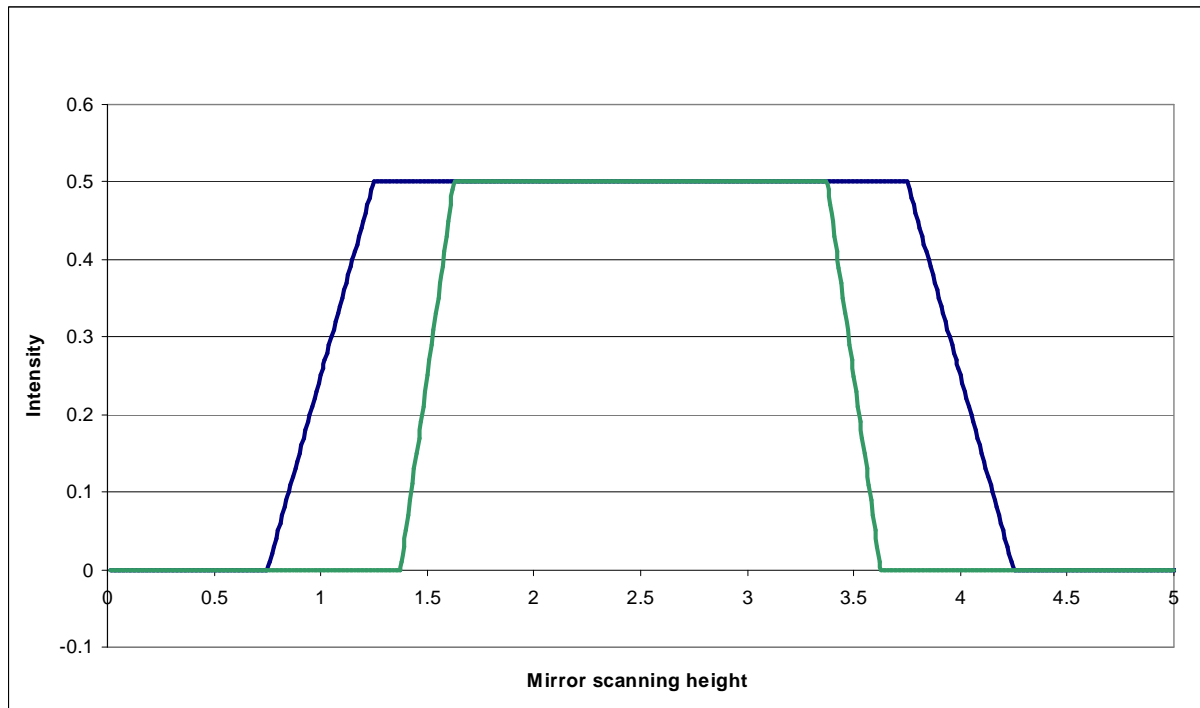
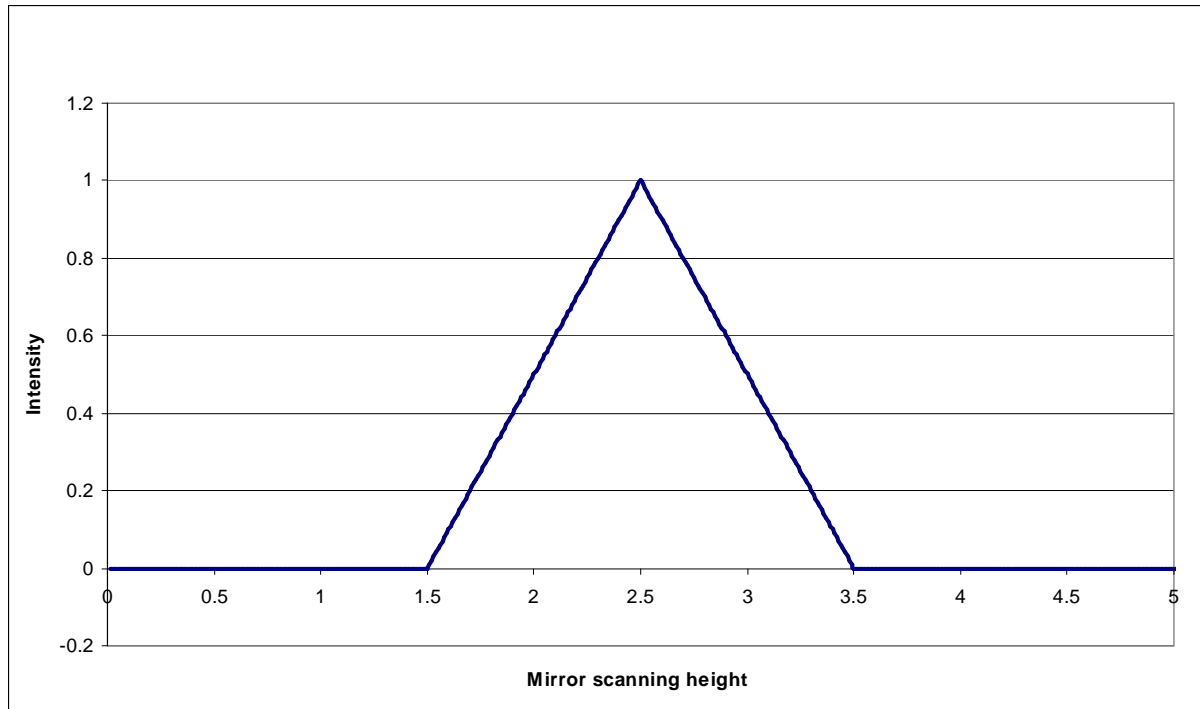


Figure 2.1e – The green trace represents a diode which is too small –  $\alpha = 3$  mrad,  $h = 4$ mm,  $y_d = 8$ mm. The FWHM is much smaller than the true value in blue.

The second is that the beam must be smaller than the transverse projection of the mirror, ie  $D < L \sin \alpha$ . If  $D > L \sin \alpha$  then the beam covers the whole mirror at once, and the FWHM of the trace gives the width of the beam, rather than any information about the angle. When approaching the limit, the top hat will become increasingly smaller, until at  $D = L \sin \alpha$  there is only a single point at maximum intensity (Fig 2.1f).



**Figure 2.1f – A trace at  $\alpha = 1$  mrad, with the beam diameter of 1mm being equal to the transverse projection of the mirror.**

Considering these constraints and the range of values required for the XFEL, a photodiode of height 10mm with its centre at 8mm, positioned 50cm behind the mirror ( $d=1m$ ) would be able to measure full traces for the entire angular range. This coordinate system assumes a movement range of 5mm starting at 0mm, and the beam centred at 2.5mm. In this case, the diode does not need to have a fine resolution on its range of motion, just positions in and out of the beam.

For a mirror length of 1m, an increment of  $10 \mu\text{rad}$  corresponds to a change in the FWHM of the trace of 0.01mm. As a result, the motion of the mirror must be accurate to  $5 \mu\text{m}$  over the 5mm range of motion. A system with these properties has already been implemented at FLASH [5]. Another constraint is the beam diameter required, which should ideally be less than 0.6mm at the mirrors. For alignment, only a single undulator segment will be used, which has a beam divergence of  $14.7 \mu\text{rad}$  as a worst case scenario. The schematic earlier shows a distance of 30m between the slit and the second mirror, so a slit size of 0.1mm would be sufficient.

### *2.1.2. Experimental demonstration*

This method was tested using a laboratory demonstration, with the setup shown in Fig. 2.1g. An optical laser with a beam diameter of 4mm was used, with two lenses (of focal lengths 50mm and 150mm) acting as a telescope, producing a collimated beam of 1.33mm diameter. This was then reflected off a 25mm long mirror, mounted on an angular stage with resolution 5 arcmin ( $0.083^\circ$ ), which was in turn mounted on a linear stage with resolution 0.01mm over a range of 25mm. The reflected light was then incident upon a photodiode with a square active area of 3.6mm side, and the photocurrent was read by a multimeter.



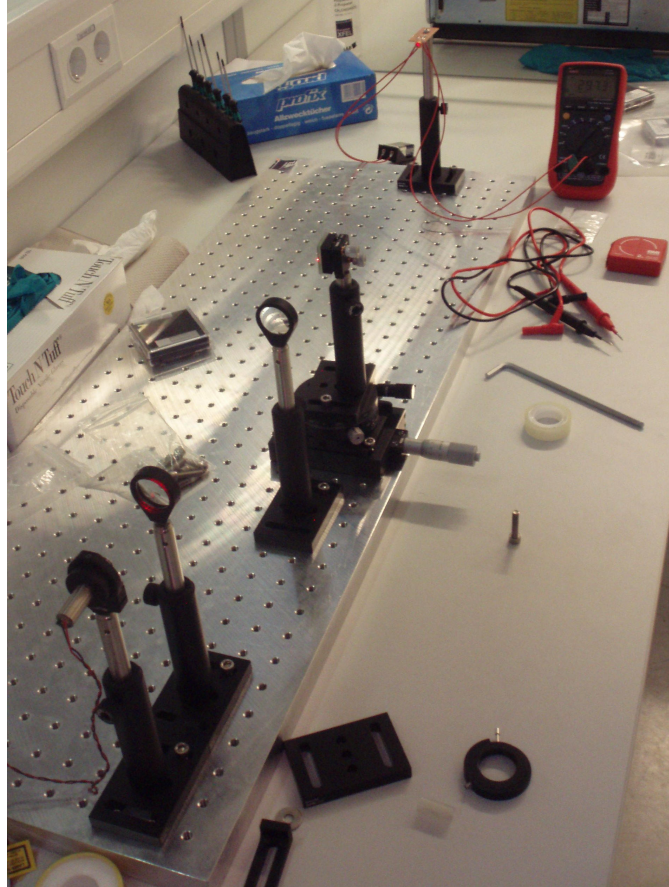


**Figure 2.1g – Laboratory demonstration of the pencil beam setup.**

The mirror was scanned across the full range of non-zero current using the micrometer screw on the linear stage, with readings taken from the multimeter every 0.05mm. This was tedious, but in the XFEL the entire motion will be computerised, meaning that it will be more accurate and enable the user to get on with something else! The traces produced are shown in Fig. 2.1h-i. Due to the limitations set out in section 2.1.1, the range of angles that could be accurately measured was 3–4.2°, so there were only two traces that could be obtained with the setup. The measured angle refers to the value read from the angular stage, while the calculated angle is that obtained from the FWHM of the trace.

It should be noted that these traces are more rounded than the theoretical examples. This is because the demonstration was carried out with a circular beam, whereas the examples were calculated for a square beam. As the measurement is taken across the entire width of the circle, it obviously has maximum intensity across the centre decreasing to the edges, causing the rounding off of the edges of the curves.

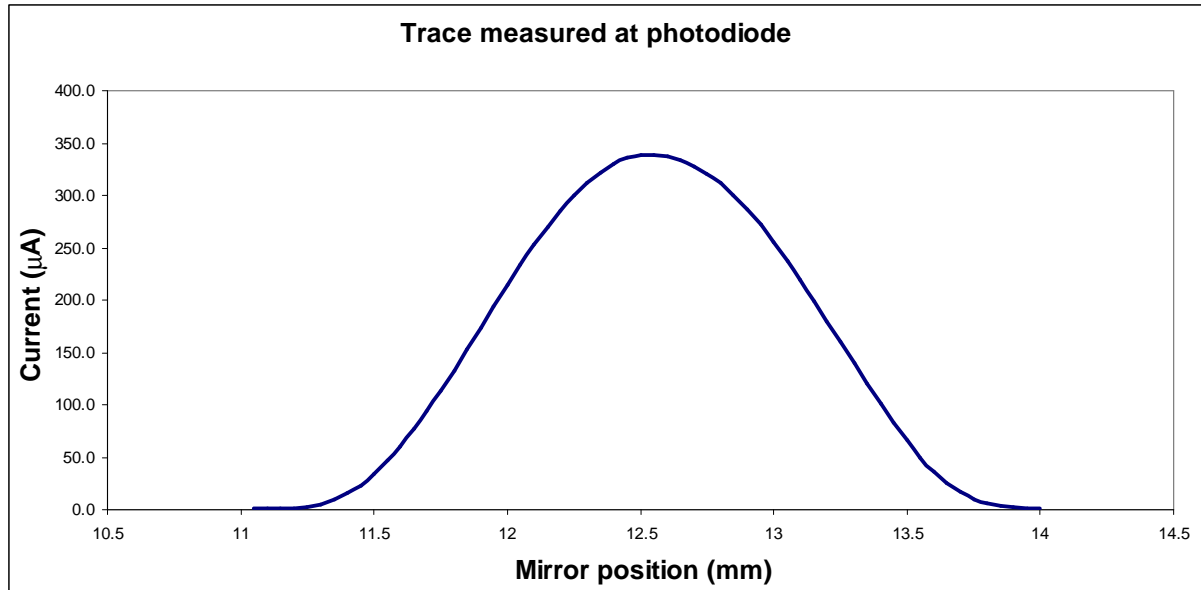


**Figure 2.1h – Measured angle = 3.13 mrad. Calculated angle = 3.06 mrad. The lack of a top-hat shows that the beam diameter is very close to the size of the transverse projection of the mirror.**

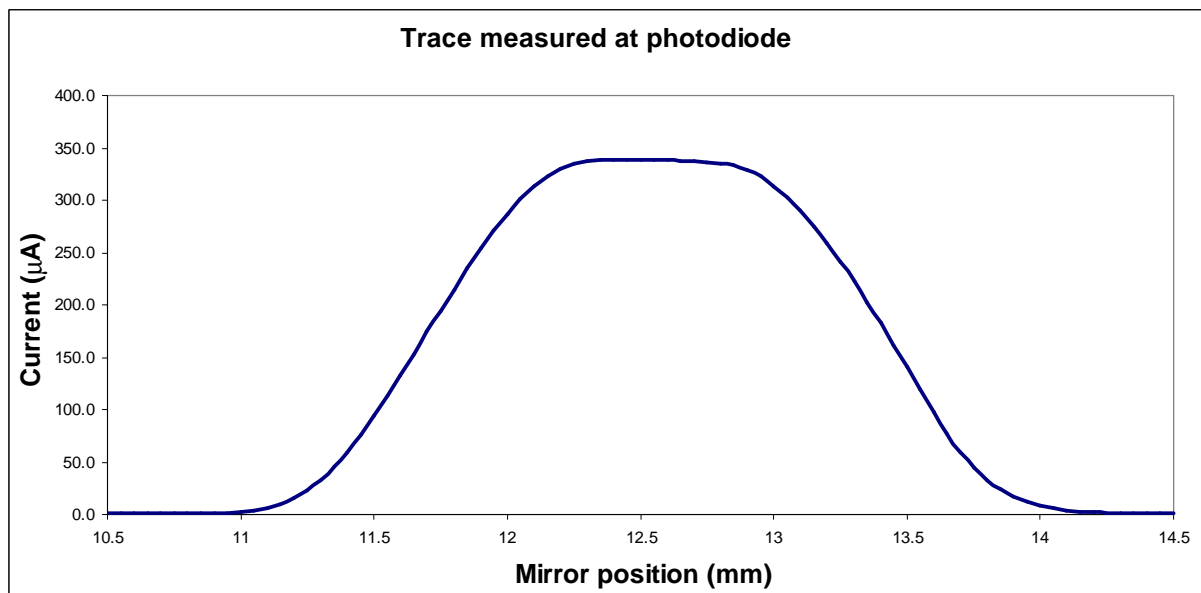


**Figure 2.1i – Measured angle = 4.33 mrad. Calculated angle = 4.00 mrad. There is an evident top hat, although the diode was slightly too small, causing an inaccurate FWHM.**

## 2.2. 'Immersion' setup with screen

An alternative scheme is to immerse the mirror in a wide beam. In this case, part of the beam will pass by the top of the mirror unreflected, and part of it will be reflected by the mirror (the bottom part is blocked by the support structure for the mirror). By placing a fluorescent screen at a certain distance behind the mirror, these images can be detected. By measuring the distance between them, the angle of the mirror can be determined.

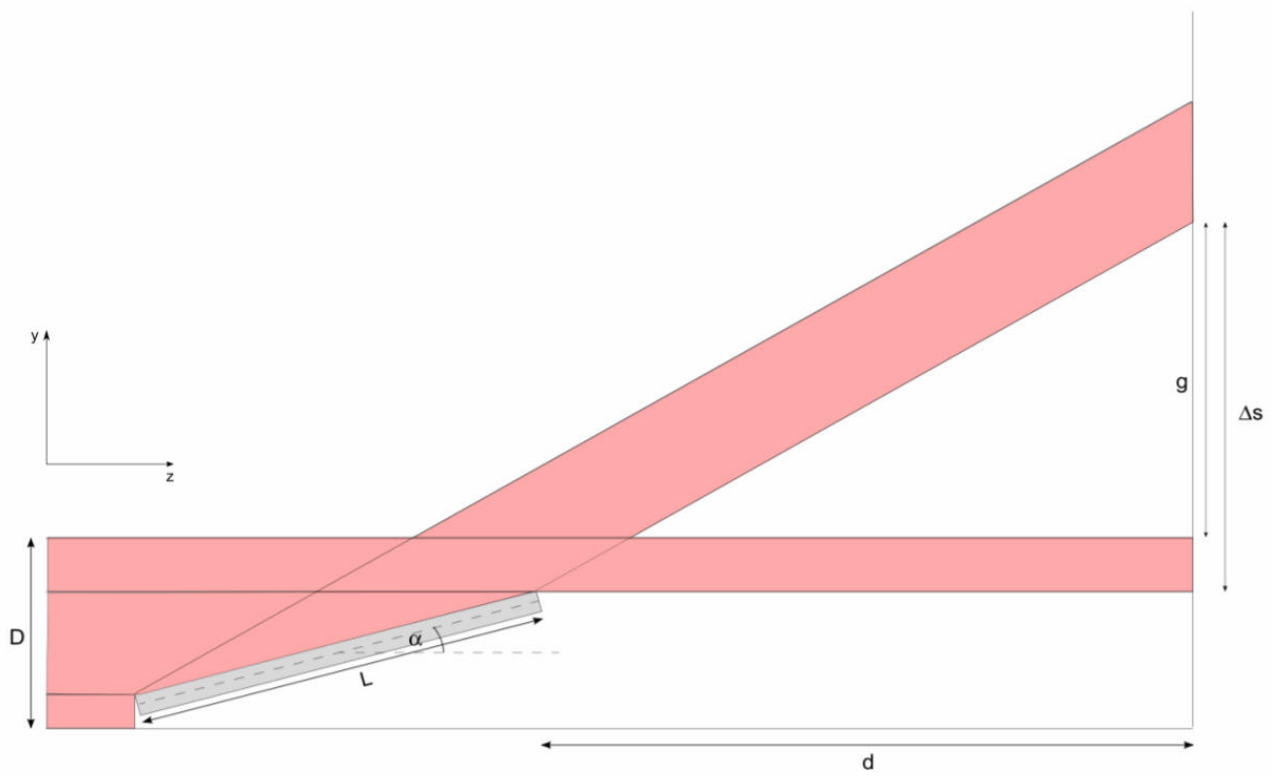


Figure 2.2a – A schematic for the immersion setup.  $D$  is the diameter of the beam,  $L$  is the length of the mirror,  $\alpha$  is the angle of the mirror,  $d$  is the distance from the far edge of the mirror to the screen (this is different to 2.1a),  $g$  is the gap between the images, and  $\Delta s$  is the distance between the bottom edges of the two images.

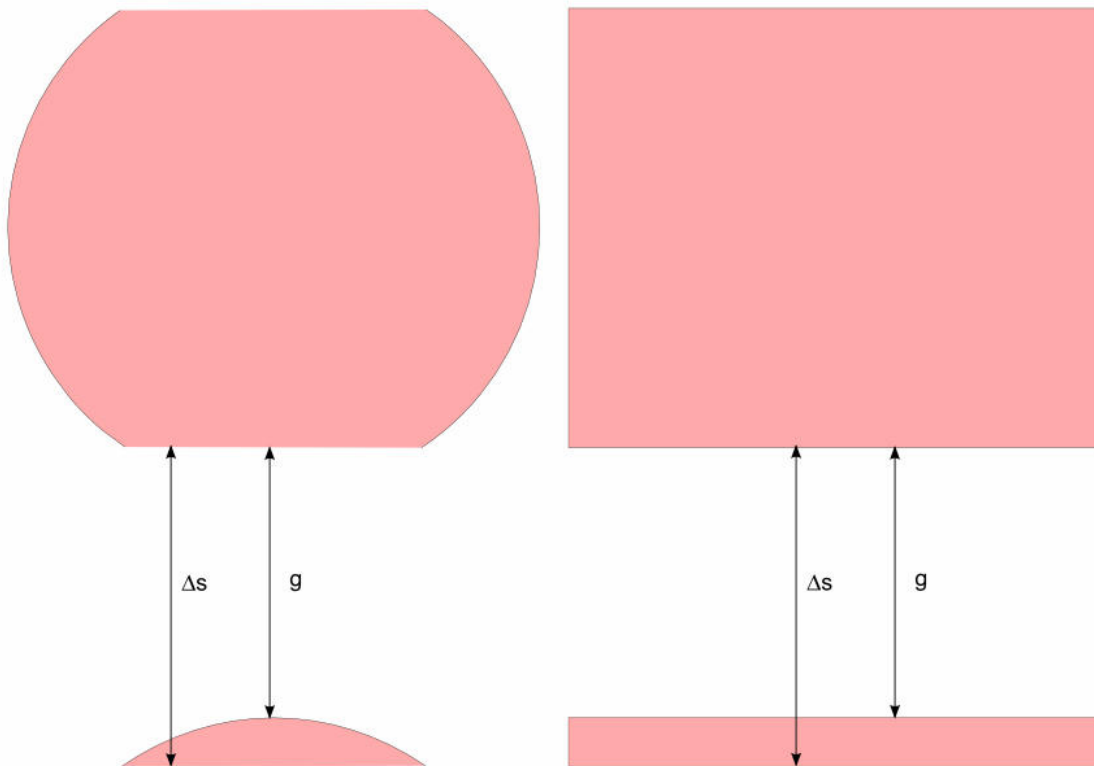


Figure 2.2b – Screen patterns for a circular and a square beam. Whilst  $\Delta s$  is easy to read from both patterns, it is very difficult to ensure that the value of  $g$  is accurate from the circular beam.

### 2.2.1. Theory for XFEL

When viewing the light on a screen, a pattern such as those shown in Fig. 2.2b will be observed. The most important measurement is  $\Delta s$ . This is the difference in path between the beam reflected from the top edge of the mirror and the unreflected beam passing just over the top of it. Noting that the angle of deviation is  $2\alpha$ , the angle of the mirror can be calculated from  $\tan 2\alpha = \frac{\Delta s}{d}$ . Once the angle is known, the value of the gap,  $g$ , can be used to determine whether the mirror is centred in the beam. This is possible using the equation  $g = 2d \tan \alpha - 0.5(D - L \sin \alpha)$ . If the value is too small, the mirror is too low in the beam and needs to be moved up, and the opposite if the value is too high.

If the screen is placed at a distance of 2m from the end of the mirror, the value of  $\Delta s$  changes by 40 $\mu$ m for each 10  $\mu$ rad increment in the mirror angle. As a result, the resolution of the screen should ideally be around 20 $\mu$ m. In order to display the entire pattern for angles up to 3 mrad, the screen must be 20mm tall, with its bottom edge aligned with the bottom of the incident beam. The choice of the screen material should be chosen consequently, remembering that the material must not be damaged by the high intensity x-rays. Ce:YAG (Cerium-doped Yttrium Aluminium Garnet) is a suitable material. However, it seems that will be difficult to manufacture a screen to of this size to give the required resolution.

Another downside is that a camera will be required to view the pattern on the screen. This is going to be quite big and cumbersome, which could pose a problem for its positioning to see be able to view the screen inside the UHV (ultra high vacuum) chamber. However, this system has been successfully implemented at LCLS, with a reported relative accuracy of 1%.

### 2.2.2. Experimental demonstration

The demonstration used the same equipment as in section 2.1.2, although in a different setup, shown in Fig. 2.2c. The lenses were used as an ‘anti-telescope’ to produce a wide non-diverging beam of diameter 12mm, and a screen containing mm-scale rulers was printed off the computer to view and measure of the pattern of the light. The mirror was mounted on the angular stage, which in turn was mounted on the linear stage, which was only adjusted to aid alignment.

To take the measurements, the angle was incremented by 0.5° and the coordinates of the edges of the two images recorded. From this, the height of the reflected image and the value of  $\Delta s$  was calculated and compared to the predicted theoretical results. Fig. 2.2d shows the divergence between the predicted and measured results.

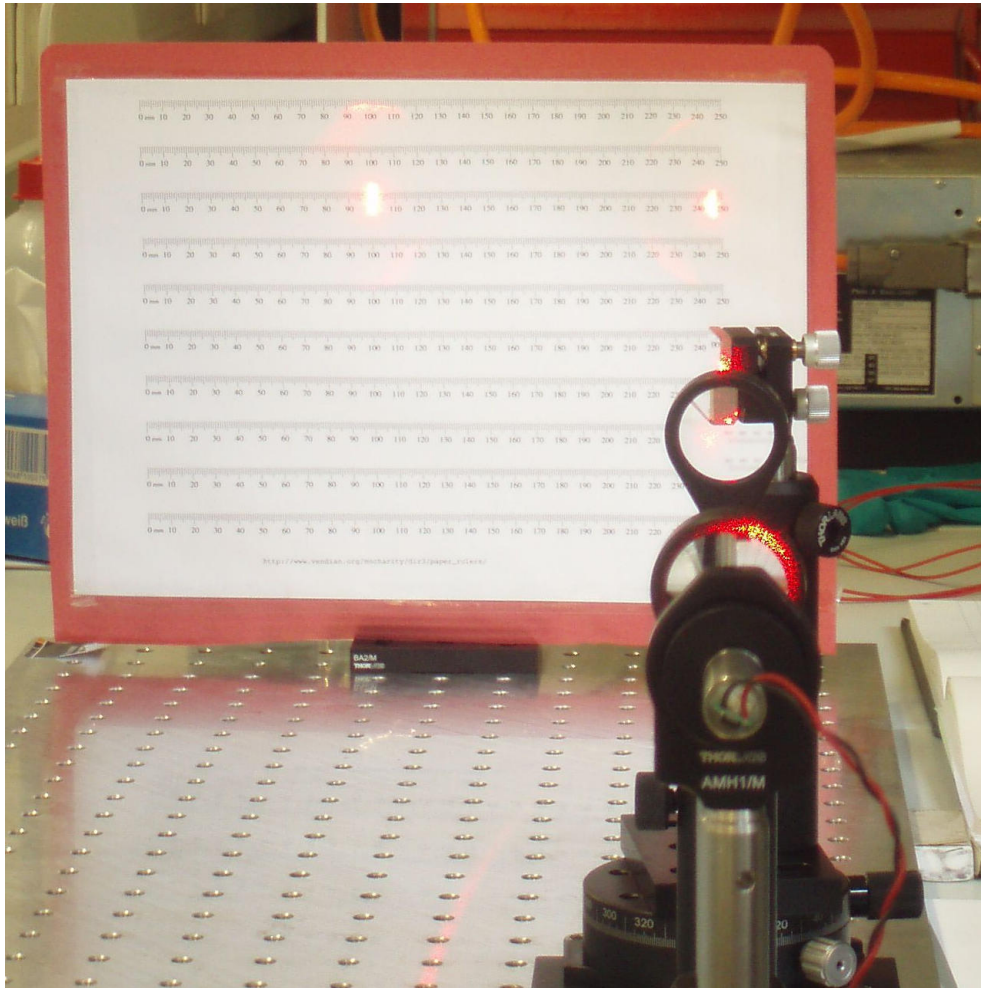


**Figure 2.2c – A view of the path of the laser through the experimental demonstration for the immersion setup using a screen. The laser beam is widened using two lenses before being partially reflected by the mirror, producing two images on the screen.**

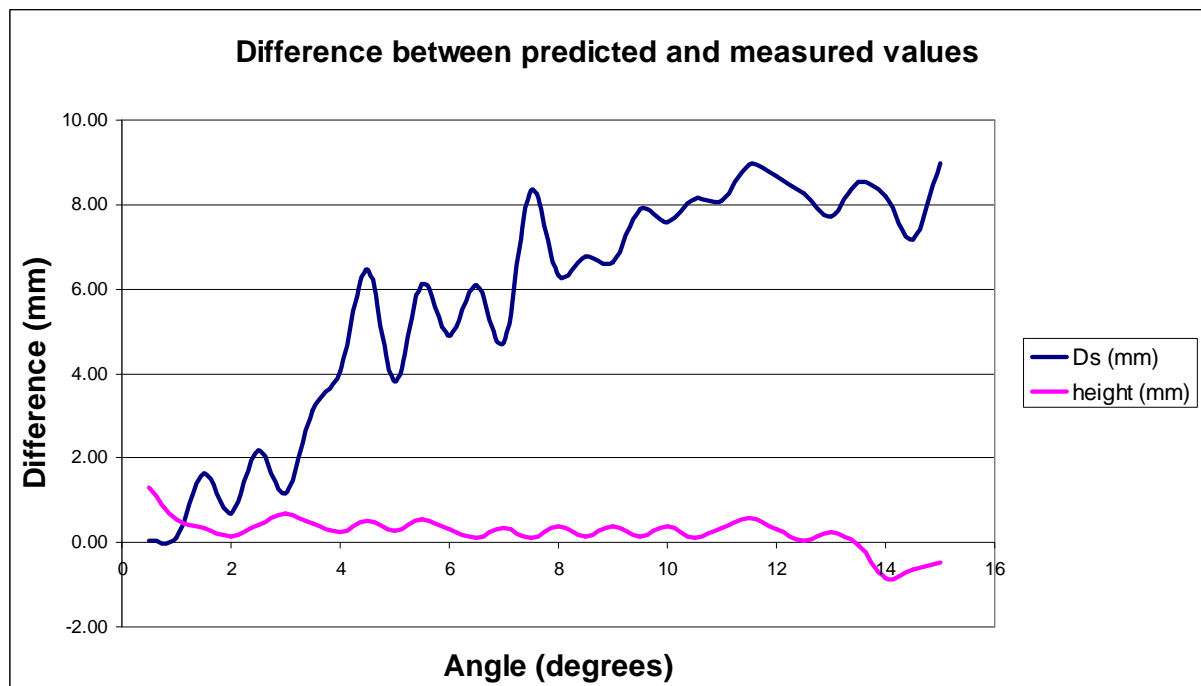


**Figure 2.2d – A graph of the (measured – predicted) value of  $\Delta s$  and height. The discrepancy increased with increasing angle, but the height of the reflected image was approximately correct at all angles.**

The results at angles below  $1^\circ$  were unreliable, as there was a very obvious diffraction pattern on the reflected image (this accounts for the very large height discrepancy at low angles). The discrepancy between the expected and measured value of  $\Delta s$  increases with angle, and this likely to be due to a misalignment of the centre of the mirror with the rotation axis of the stage. However, despite several attempts, this alignment could not be improved. The cause of this discrepancy is still unclear. If the beam was slightly converging, it would cause the measured values to be too large, but when the mirror was removed, the beam appeared to be the same size across the full length of the breadboard.

### 2.3. 'Immersion' setup with photodiode

It is unclear whether a screen of the necessary resolution will be available for use in the XFEL, so another scheme was considered; to scan a long, narrow diode across the image plane where the screen sat in section 2.2. This is in the same geometry as illustrated in Fig. 2.2a, but instead of viewing the pattern directly, a trace would be visible from the motion of the diode. If the diode was sufficiently narrow, the edges of the images should be easily determined, allowing the distances highlighted in section 2.2.1 to be calculated.

#### 2.3.1. Theory for XFEL

The most important piece of theory is to determine whether the diode will provide an accurate representation of the pattern produced by the mirror.

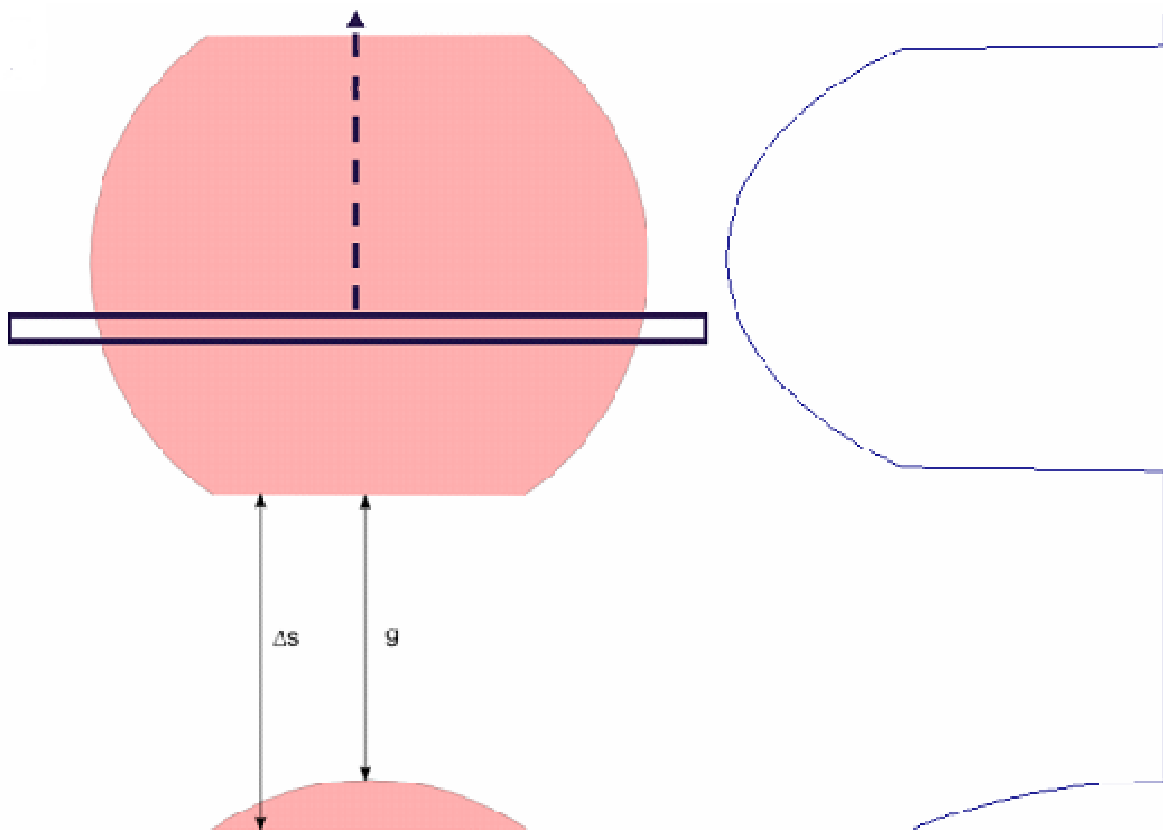


**Figure 2.3a – Trace seen by a narrow photodiode scanning the pattern from a circular beam. The bottom edges of the two images should give identical intensities, and have sharp peaks so they are easy to identify. However, at the top of the bottom image, the intensity goes to zero gradually and the exact edge may be difficult to determine.**

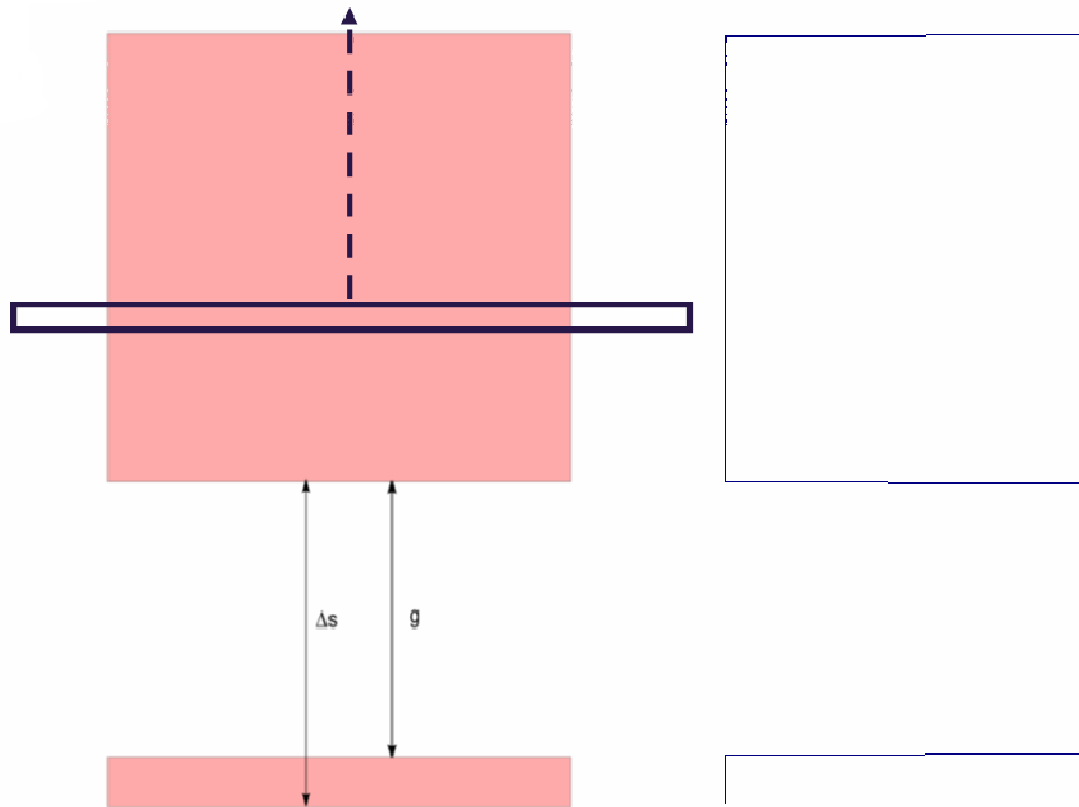


**Figure 2.3b – Trace seen by a narrow photodiode scanning the pattern from a square beam. In contrast to the circular beam, all the edges are sharp and easy to find.**

If the diode is  $10\mu\text{m}$  tall, even a motion with an accuracy of  $10\mu\text{m}$  should be accurate enough to determine the edges of the trace to the required resolution, assuming the diode scans the same plane that the screen was in section 2.2. The production of a diode which is only  $10\mu\text{m}$  high but up to  $1\text{cm}$  wide is not trivial and an investigation into whether this is possible must be carried out. The downside to this scheme is that this is an extra degree of freedom that is required, and the trace is not quite as simple to read as a pattern on a screen, especially if a circular beam is used.

### 2.3.2. *Experimental demonstration*

An experimental demonstration in the style of those for the previous two schemes was attempted. The only change between this and the setup described in section 2.2.2 was that the screen was replaced by the linear stage with the photodiode mounted on top of it. However, it was not as easy to implement for a number of reasons.

Firstly, to recreate a narrow diode, the intent was to place a slit in front of the diode to reduce its active area. However, the slit could not be firmly attached to the linear stage along with the photodiode in a way that it was blocking out the same portion of the beam at all positions in the image plane. Also, as only a small portion of the beam was reflected to begin with, the current measured was well below the  $340\mu\text{A}$  maximum. By placing a small slit in front of the photodiode, this was reduced to only  $2\text{--}3\mu\text{A}$ , with background light of  $1.2\pm 0.3\mu\text{A}$ . This would not give a readable trace.

Therefore, the experiment was carried out using the full ( $3.6\text{mm}$ ) active area of the diode. The data is shown in Figs. 2.3c and 2.3d.

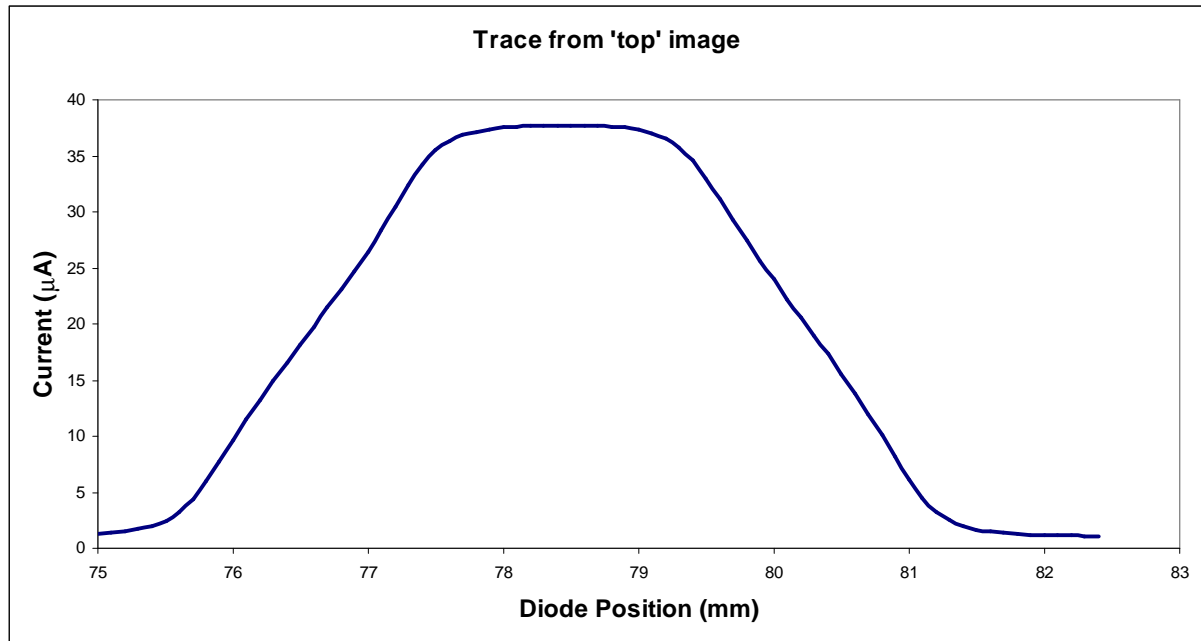


**Figure 2.3c – Trace from region of reflected image. The trace is not identical to the shape seen in the top of Fig. 2.3a due to the large size of the diode, which rounds out the edges. The bottom edge of the area can be found by taking the point where the maximum of intensity drops off (79.3mm) and subtracting the diode height (3.6mm) to get 75.7mm.**



**Figure 2.3d – Trace from region of unreflected image. The bottom edge of the image is at 9.3mm, giving  $\Delta s = 66.4\text{mm}$ , which is about 3mm smaller than expected for an angle of  $5^\circ$ . The top of the image is much harder to find, as it is not the peak (due to the circular nature of the beam, the current is decreasing before the peak is reached), and the right edge of the trace goes to zero fairly slowly.**

This experiment was not accurate. The circular beam made the edges difficult to determine from the trace, but the biggest source of error was due to the relatively small (25mm) range of motion of the linear stage. This meant that the stage had to be moved on the breadboard between taking the traces, which involved removing the photodiode from the stage, moving the stage, and remounting the photodiode, causing scope for misalignment. When the experiment was repeated, this was found to produce an error of up to 5mm in  $\Delta s$ , equivalent to  $0.5^\circ$ , much worse than the required resolution.



### 3. Comparison of Alignment Methods

Now that all three schemes have been considered, all that remains is to compare them, which is done in table 3.1.

|                     | Pencil beam  | Immersion – screen   | Immersion – diode  |
|---------------------|--|--|--|
| Degrees of freedom  | Mirror y-position adjustment<br>Mirror angular adjustment<br>In/out positioning of diode   | Mirror y-position adjustment<br>Mirror angular adjustment<br>In/out positioning of screen  | Mirror y-position adjustment<br>Mirror angular adjustment<br>Fine adjustment of photodiode y-position  |
| XFEL Implementation | If diode is placed 50cm behind the far edge of the 1m long mirror, a diode of height 10mm will be able to see the full, accurate traces for all of the required angles (1–3 mrad).<br>The required range of y-motion for the mirror is 5mm.<br>The beam diameter must be less than 1mm to satisfy the necessary condition to give a top-hat trace ( $D < L \sin \alpha$ ).<br>Smaller beam = better image. | If the screen is placed 2m behind the far edge of the 1m long mirror, a screen of height 20mm would be able to see both image patterns for all the required angles (1–3 mrad), for a 4mm beam diameter.<br>A 4mm square slit should be used to make it easier to define the edge of the images (the point of a circle is hard to find).<br>The main difficulty with this setup is the fact that a camera must be installed to see the image on the screen. | If the diode is placed 2m behind the far edge of the 1m long mirror, a scanning range of 20mm would be able to see both image patterns for all the required angles (1–3mrad), for a 4mm beam diameter.<br>A square slit should be used for the beam, as this will make the trace a lot sharper, with defined edges and top-hats.<br>A small slit (10 $\mu$ m) will give a clearer definition of the edges of the areas on the trace. |
| Accuracy            | As the photodiode is fixed, the required resolution is in the movement of the mirror. For a resolution of 10 $\mu$ rad, must be able to measure FWHM to 0.01mm, which means a resolution of mirror motion of 0.005mm (5 microns). This has already been achieved at FLASH  | For a resolution of 10 $\mu$ rad, $\Delta s$ must be measured to within 40 $\mu$ m at a distance of 2m. This means that the screen must have a resolution of 20 $\mu$ m at worst.<br>It could be difficult to find a screen that matches this specification.   | For a resolution of 10 $\mu$ rad, $\Delta s$ must be measured to within 40 $\mu$ m at a distance of 2m. Must be ~1cm long to measure entire pattern width. With a 10 $\mu$ m high diode, this is achievable, assuming there are no issues with the intensity of the x-ray beam.  |
| Ease of use         | Easy to read FWHM off trace.   | Easy to measure distances off screen.  | If a small diode is used, it will be easy to find the image edges and hence make the necessary measurements.   |
| Conclusion          | Easy to install and read, and ensure the necessary accuracy.   | Easiest to read, and quick, but hard to achieve the required resolution.   | Should give good resolution, but untested in lab. An extra moving part is a downside.  |

**Table 3.1 – A comparison of the three alignment schemes considered.**

In conclusion, the ‘pencil beam’ scheme should work the best. The next consideration is how it can be implemented, but it seems that placing a 10mm high diode in and out of the beam path should be fairly simple. A suitable detector could be a Passivated Implanted Planar Silicon (PIPS) Detector produced by CANBERRA [6]. Producing a slit system for a 0.1mm x-ray beam may be the limiting factor on whether this can be used or not, with considerations to be made about the heat load applied to such a system.

## 4. Acknowledgements

I would like to thank my supervisor, Dr. Jan Grünert for all of the guidance he has given and wisdom he has shared with me for the duration of my project. I would also like to thank the other member of WP-74, Wolfgang Freund, for his help in procuring the apparatus for the demonstrations and in assembling the electronics. Finally, I'd like to thank the members of WP-73, in particular Harald Sinn, for supervising me while the rest of my work package was on holiday!

## 5. References

1. M. Dohlus, DESY Summer Student Lecture on FELs, 2010 (<http://www.desy.de/f/students/lectures2010/dohlus.pdf>).
2. European XFEL Technical Design Report, Chapter 6: Photon Beamlines and Scientific Instruments, 2007.
3. European XFEL website – “In Comparison” ([http://www.xfel.eu/overview/in\\_comparison](http://www.xfel.eu/overview/in_comparison))
4. H. Sinn, European XFEL WP-73 Presentation, 2010
5. S. Pauliuk et al, “A Fast Switching Mirror Unit for FLASH”, EPAC '08 Proc., 2008.
6. CANBERRA PIPS detectors data sheet (<http://www.canberra.com/products/1084.asp>)